Published in final edited form as:
Cancer Cell. 2008 December 9; 14(6): 458–470. doi:10.1016/j.ccr.2008.11.003.

Akt determines replicative senescence and oxidative or oncogenic premature senescence and sensitizes cells to oxidative apoptosis

Veronique Nogueira[1], **Youngkyu Park**[1], **Chia-Chen Chen**[1], **Pei-Zhang Xu**[1], **Mei-Ling Chen**[1], **Ivana Tonic**[1], **Terry Unterman**[2,3], and **Nissim Hay**[1,*]

[1]Department of Biochemistry and Molecular Genetics, University of Illinois at Chicago, Chicago, Illinois 60607 USA

[2]Department of Medicine University of Illinois at Chicago, Chicago, Illinois 60607 USA

[3]Jesse Brown VA Medical Center, Chicago, Illinois, 60612 USA

Summary

Akt-deficiency causes resistance to replicative senescence, oxidative stress- or oncogenic Ras-induced premature senescence, and to reactive oxygen species (ROS)-mediated apoptosis. Akt activation induces premature senescence and sensitizes cells to ROS-mediated apoptosis by increasing intracellular ROS through increased oxygen consumption and by inhibiting the expression of ROS-scavengers downstream of FoxO, particularly sestrin3 expression. This uncovers an Achilles' heel of Akt, since in contrast to its ability to inhibit apoptosis induced by multiple apoptotic stimuli; Akt could not inhibit ROS-mediated apoptosis. Furthermore, treatment with rapamycin that led to further Akt activation and resistance to etoposide, hypersensitized cancer cells to ROS-mediated apoptosis. Given that rapamycin alone is mainly cytostatic, this constitutes a strategy for cancer therapy that selectively eradicates cancer cells via Akt activation.

Introduction

The serine/threonine kinase Akt is activated by extracellular signals that activate phosphatidylinositol 3-kinase (PI3K), which generates PI (3,4,5) P3 (PIP3). Akt activity is negatively regulated by phospholipids phosphatases that negate the activity of PI3K, such as the tumor suppressor PTEN. In mammalian cells, there are three separate genes encoding the three mammalian Akt isoforms (Akt1-3). Akt activity is also downregulated by the

*To whom correspondence should be addressed: University of Illinois at Chicago Department of Biochemistry and Molecular Genetics (M/C 669) College of Medicine 900 S. Ashland Ave. Chicago, Illinois 60607 Tel: 312-355-1684 Fax: 312-355-2032 nhay@uic.edu.

Significance

Oncogenic and oxidative stress - induced senescence attenuates tumorigenesis. Here we show that Akt mediates this premature senescence. Akt exerts its effect on senescence by elevating intracellular ROS. The elevation of ROS induced by Akt also sensitizes cells to ROS-mediated cell death, and therefore can be exploited for cancer therapy. Hyperactivation of Akt, which is frequently occurring in human cancers, promotes resistance to chemotherapy. Here we provide a strategy that not only evades chemoresistance induced by Akt, but also selectively eradicate cancer cells that display hyperactive Akt. As a proof of concept for this strategy we showed that ROS-inducer preferentially suppresses in-vivo tumor growth of cancer cells expressing activated Akt, which is further accelerated by rapamycin.

activation of its downstream effector mTORC1, which in turn induces a negative feedback mechanism that inhibits Akt activity (reviewed in (Bhaskar and Hay, 2007)).

Hyperactivated Akt provides both protection from apoptosis and uncontrolled cell cycle progression (Kandel et al., 2002)- two major prerequisites for cancer susceptibility, and this may explain, at least in part, its frequent activation in human cancers (reviewed in (Bhaskar and Hay, 2007)). However, the most evolutionarily conserved function of Akt is in the control of energy metabolism, which in mammalian cells, is coupled to its ability to inhibit apoptosis and to promote cell cycle progression (reviewed in (Plas and Thompson, 2005; Robey and Hay, 2006).

The coupling between energy metabolism and lifespan is well documented, and calorie restriction was shown to extend lifespan in a wide spectrum of organisms. Attenuated insulin signaling through PI3K and its downstream effector, Akt, is associated with a decline in energy metabolism and an increase in lifespan. In C. elegans, increased lifespan associated with impaired PI3K/Akt signaling requires the presence of the forkhead transcription factor DAF-16. There are 4 mammalian homologues of DAF-16: FOXO1, FOXO3a, and FOXO4, and FOXO6 (Greer and Brunet, 2005). Akt directly phosphorylates DAF-16 and its mammalian homologues and this phosphorylation excludes them from the nucleus thereby inhibiting their transcriptional activity (Greer and Brunet, 2005). Thus, the activity of DAF-16 and its mammalian homologues is increased when Akt activity is reduced.

The accumulation of somatic damage is considered a major determinant of lifespan both at the organismal and cellular levels. This damage is mainly caused by the accumulation of reactive oxygen species (ROS) (Chance et al., 1979), which are natural by-products of oxidative energy metabolism. Damage induced by ROS including, DNA lesions, protein oxidation, and lipid per oxidation, is determined by both the rate of energy metabolism and the activity of ROS scavengers such as superoxide dismutase (SOD) and catalase that degrades hydrogen peroxide. Multiple experiments showed that ROS play a critical role in determining lifespan and cellular senescence of mammalian cells (reviewed in (Balaban et al., 2005). The senescence of mouse embryo fibroblasts (MEFs), having long telomeres, is likely to occur via accumulation of ROS when are grown at ambient oxygen levels (Parrinello et al., 2003). Consistently earlier observations showed that human diploid cells undergo senescence at lower rate under low-oxygen conditions (Packer and Fuehr, 1977).

Here we provided genetic evidence that Akt determines replicative senescence of mammalian cells in culture, and mediates premature senescence induced by activated Ras or oxidative stress. Additionally, Akt activation is sufficient to induce premature senescence. In the course of these studies we found that Akt also sensitized cells to ROS-mediated apoptosis. We showed that Akt exerts its effect by increasing intracellular levels of ROS through an increase in oxygen consumption and the inhibition of FoxO transcription factors.

Despite its ability to inhibit apoptosis, Akt could not protect against ROS-mediated cell death but rather sensitized cells to this cell death. Thus, we uncovered the Achilles' heel of Akt, which can be exploited for cancer therapy to selectively kill cancer cells with hyperactive Akt. Most importantly, we showed that rapamycin, which is usually cytostatic, sensitized cells to ROS-mediated cell death because it also activates Akt via the inhibition of a negative feedback loop (Bhaskar and Hay, 2007; Harrington et al., 2005; Hay, 2005). Thus, by combining rapamycin and a ROS-inducer, it is not only possible to evade chemoresistance mediated by Akt activation, but also to selectively kill cancer cells with hyperactive Akt. In addition, our demonstration that rapamycin treated cells are sensitized to

ROS-induced cell death provides a strategy that would substantially increase the efficacy of rapamycin treatment.

Results

Akt regulates cellular lifespan

We used wild-type (WT) or Akt1 and Akt2 double knockout (Akt1/2 DKO) MEFs to determine the role of Akt in the regulation of cellular lifespan. MEFs were subjected to 3T3 protocol to calculate population doubling (PDL). Senescence-associated β-galactosidase (SA–β-Gal) staining and bromodeoxyuridine (BrdU) incorporation were used as readouts for senescence. As shown in Figure 1A, WT MEFs began senescing after passage 13, whereas Akt1/2 DKO MEFs began senescing after passage 16. This was also confirmed by the enlarged and flattened cell morphology (not shown), by SA-β-Gal staining (Figure 1B) and by BrdU incorporation (Figure 1C). Notably, we have previously shown that Akt1/2 DKO cells divide slower than WT cells (Skeen et al., 2006); therefore, we passaged the cells every 5 days instead of every 3 days. As shown in Figure 1D the senescence of Akt1/2 DKO still lagged behind WT MEFs. These results provided evidence that Akt determines the cellular lifespan and replicative senescence of MEFs.

The results obtained with MEFs were corroborated using human foreskin diploid fibroblasts (HDFs). The knockdown of Akt1 alone in HDFs minimally impaired proliferation rate but markedly attenuated cellular senescence as measured by population doublings (Fig. S1A).

Akt regulates cellular lifespan and intracellular ROS levels by mediating oxygen consumption and inhibiting FoxO transcription factors

MEFs, and to some extent HDFs, lifespan in culture is coupled to oxygen consumption and intracellular ROS (Parrinello et al., 2003). We therefore determined the role of Akt in these two parameters. Oxygen consumption was impaired in Akt1/2 DKO cells (Figure 2A) and was accelerated in cells expressing activated Akt (Figure 2B) or in Pten-/- cells (Figure 2C). We next determined whether Akt could affect intracellular levels of ROS, and found that Akt1/2 DKO MEFs had significantly lower ROS levels compared with WT MEFs (Figure 2D), whereas cells expressing activated Akt (Figure 2E) and Pten-/- cells (Figure 2F) had significantly higher levels of ROS. These results show that Akt regulates intracellular ROS levels. We had previously shown that activation of Akt increases ATP production by both glycolysis and oxidative phosphorylation (Gottlob et al., 2001). Because ROS are byproducts of oxidative phosphorylation, Akt-induced ROS levels could be dependent, in part, on Akt-mediated oxygen consumption. To show that the decrease in oxygen consumption in Akt1/2 DKO MEFs correlates with a decrease in ROS production, we substituted glucose with galactose in the cell culture media. This substitution decreases the generation of ATP from glycolysis, forcing cells to increase respiration (Rossignol et al., 2004; Warburg et al., 1967). Indeed, the substitution of glucose with galactose increased oxygen consumption in Akt1/2 DKO MEFs with concomitant increase in ROS generation (Fig. S2A, B). These results provided indirect evidence, suggesting that the decrease in oxygen consumption in Akt1/2 DKO MEFs contributes to the reduced ROS levels.

To exclude the possibility that the reduced ROS levels observed in Akt1/2 DKO MEFs is due to the decrease in their proliferation rate, we first, immortalized both WT and Akt1/2 DKO MEFs with SV40 large T. The SV40 large T-immortalized WT and Akt1/2 DKO MEFs proliferate at a similar rate (Fig. S2C), yet the Akt1/2 DKO MEFs still display decreased oxygen consumption and ROS levels (Fig. S2D, E). Second, when WT and Akt1/2 DKO MEFs were grown to confluency and stopped dividing (Fig. S2F), oxygen consumption and ROS levels remained reduced in Akt1/2 DKO MEFs (Fig S2 G,H). Thus,

these results indicate that the reduced ROS level in Akt1/2 DKO MEFs is not a consequence of their attenuated proliferation.

Because FoxO transcription factors are downstream effectors of Akt, and have a conserved role ROS regulation, via the regulation of detoxifying enzymes (Greer and Brunet, 2005), we examined the contribution of FoxO to the reduced ROS levels in Akt1/2 DKO MEFs. FoxO transcriptional activity is elevated in Akt1/2 DKO MEFs (Fig. S3). Consistently, both the levels of MnSOD and catalase, two known targets of FoxO (Kops et al., 2002; Nemoto and Finkel, 2002), were elevated in Akt1/2 DKO MEFs (Fig. 3A). Moreover, when dominant-negative FoxO1 (DN-FoxO), containing only its DNA binding domain, was expressed in Akt1/2 DKO cells, MnSOD and catalase levels were reduced to their levels in WT cells, although we did not find a further decrease in the levels of these enzymes in WT cells expressing DN-FoxO. Importantly, we have identified an additional mechanism by which FoxOs could affect intracellular ROS levels. We found that sestrin3 (Sesn3) expression is highly induced by activated FoxO (Fig. 3G). The ability of FoxO to elevate Sesn3 RNA and protein is conserved in rodent and human cells (C.C.C and N.H, data not shown). Sesn3 is a member of a family of proteins, which also include sestrin1 (Sesn1) and sestrin2 (Sesn2). All three members had been shown to decrease intracellular ROS and to confer resistance to oxidative stress (Kopnin et al., 2007), probably by regenerating overoxidized peroxiredoxins that deoxidize ROS (Budanov et al., 2004). Sesn1 and Sesn2 are p53 target genes and are responsible for the resistance to oxidative stress induced by p53 both in vitro and in vivo (Budanov et al., 2002; Matheu et al., 2007; Sablina et al., 2005). Sesn3 expression is not regulated by p53 but its overexpression was shown to reduce ROS induced by activated Ras (Kopnin et al., 2007). Therefore, FoxO-induced Sesn3 expression could contribute to the regulation of intracellular ROS and to the resistance to oxidative stress. Indeed, we found that Sesn3 expression is elevated in Akt1/2 DKO MEFs (Fig. 3 H), and is reduced in FoxO3a-/- MEFs (Fig. 3 I). Furthermore, the knockdown of Sesn3 in Akt1/2 DKO cells restored ROS levels to the levels observed in WT cells (Fig. 3J). These results suggest that Sesn3 is a major regulator of intracellular ROS downstream of Akt and FoxOs. Since all the MEFs used in these studies were immortalized with DN-p53, the effect of FoxO and Akt on Sesn3 expression is clearly p53-independent. Consistent with ability of FoxO to elevate the expression of ROS-scavengers in Akt1/2 DKO MEFs, we found that DN-FoxO restored ROS levels in Akt1/2 DKO MEFs (Figure 3B).

To further assess the role of FoxO in the regulation of lifespan in culture, we utilized FoxO3a null MEFs, as FoxO3a is the major FoxO isoform expressed in MEFs (data not shown). By following replicative senescence of primary WT and FoxO3-/- MEFs, it was evident that FoxO3-/- MEFs senesced much faster than WT MEFs (Figure 3C). Furthermore, we found that FoxO3-/- MEFs senesced spontaneously after a few days in culture. When FoxO3-/- MEFs were plated at low density and were allowed to grow for 17 days, they underwent senescence whereas WT cells did not senesce (Figure 3D, E). This was correlated with the accumulation of ROS in FoxO3-/- cells when compared with WT cells (Figure 3F).

Akt-deficiency exerts resistance to premature senescence induced by oxidative stress and by activated Ras

Having determined the role of Akt and FoxO in replicative senescence, we sought to determine the role of Akt in premature senescence induced by oxidative stress. We first examined the ability of WT or Akt1/2 DKO primary MEFs to senesce upon exposure to H_2O_2. Exposure to sub-lethal concentrations of H_2O_2 increased intracellular levels of ROS in WT MEFs (Figure 4A) and decreased lifespan in culture as assessed by the enlarged and flattened cell morphology, SA-β-gal staining (Figure 4B) and BrdU incorporation (Figure 4C). In Akt1/2 DKO MEFs, however, ROS levels were markedly lower upon exposure to

H_2O_2 (Figure 4A), and likewise Akt1/2 DKO MEFs were markedly resistant to premature senescence as compared with WT MEFs (Fig 4B, C). Notably, intracellular ROS levels were continued to increase after H_2O_2 treatment (Fig 4A), and this is probably due to the activation of Akt by H_2O_2 (see Fig. 6B). The requirement of Akt for oxidative stress induced senescence was also corroborated in HDFs (Fig. S1B,C).

The resistance of Akt1/2 DKO MEFs to oxidative stress–induced senescence is abrogated by the over expression of DN-FoxO or the knockdown of FoxO3 (Figure S4 A-C). Furthermore, the knockdown of Sesn3, which is a FoxO target (Fig. 3G-I), abrogated the resistance of Akt1/2 DKO MEFs to oxidative stress-induced premature senescence (Figure 4D). Conversely, expression of activated FoxO1 in p27-/- MEFs conferred relative resistance to premature senescence (Figure S4D,E). For this experiment we used p27-/- cells to avoid cell cycle arrest induced by activated FoxO (Greer and Brunet, 2005). Similar results were obtained when p27-/- MEFs were compared with $Akt1^{-/-}p27^{-/-}$ MEFs (Fig. S4F-H). The deficiency of Akt1 in p27-/- cells was sufficient to exert resistance to H_2O_2-induced senescence, although to a less extent than observed when both Akt1 and Akt2 are deleted in the WT background. Activated FoxO reduced ROS levels and exerted resistance to H_2O_2 induced senescence in p27-/- MEFs similar to that observed in p27-/-Akt1-/- MEFs in the absence of activated FoxO (Fig. S4F-H).

Oncogenic Ras induces premature senescence of primary cells (Serrano et al., 1997), which was shown to be mediated, at least in part, via elevated intracellular ROS levels (Lee et al., 1999). We therefore examined the ability of activated Ras ($H\text{-}Ras^{val12}$) to induce senescence of Akt-deficient cells. As expected, activated Ras elevated ROS levels in WT cells, but this elevation was markedly reduced in Akt1/2 DKO MEFs (Figure 4E). Expression of DN-FoxO in Akt1/2 DKO MEFs increased ROS level that is induced by activated Ras (Fig. S5A). Consistent with previous results (Lee et al., 1999), Ras-induced premature senescence is preceded by reduced MnSOD levels (Fig. S5B) and is inhibited by the anti-oxidant N-acetyl-L-cysteine (NAC) (Fig. S5C, D). Accordingly, Akt1/2 DKO MEFs were relatively resistant to premature senescence induced by activated Ras (Figure 4F, G).

Premature senescence induced by activated Ras is dependent on p53 activation and the increase in $p19^{ARF}$, and p16 (reviewed in (Schmitt, 2007)). We therefore analyzed $p19^{ARF}$ and p16 levels, and p53 activation, as assessed by serine 15 phosphorylation of p53, in WT and Akt1/2 DKO MEFs following activated Ras expression (Figure 4H) or exposure to H_2O_2 (Figure 4I). As expected, $p19^{ARF}$ expression was elevated with concomitant activation of p53 and the induction in p16 levels in WT cells; but these were substantially diminished in Akt1/2 DKO cells. Conversely the activation of Akt, which is sufficient to induce premature senescence (Fig. 5E,F), elevated the expression of $p19^{ARF}$, p16, and the phosphorylation of p53, which were diminished in the presence of NAC (Fig. S5I). Thus, Akt-deficiency inhibits the induction of $p19^{ARF}$, and p16 and p53 phosphorylation by activated Ras or oxidative stress, while the activation of Akt is sufficient to induce $p19^{ARF}$, p53 phosphorylation, p16 and premature senescence.

The resistance of Akt1/2 DKO MEFs to premature senescence induced by activated Ras was also dependent on FoxO because activated FoxO1 increased this resistance in WT MEFs (Figure S5E, F). Consistently, we found that FoxO3-/- MEFs were hypersensitized to premature senescence induced by H_2O_2 or activated Ras (Figure 5 A-D).

Taken together these results provide compelling evidence that both oxidative stress– and activated Ras– induced premature senescence are dependent on Akt, which exerts its effect via an increase in oxygen consumption and inhibition of FoxO transcription factors.

Akt sensitizes cells to oxidative stress-induced cell death- the Achilles' heel of Akt

Exposure of immortalized MEFs, expressing DN-p53, to increasing amounts of H_2O_2, induced cell death (Fig. 6A). We expected that WT cells would be more resistant to apoptosis than Akt1/2 DKO cells. Indeed, Akt1/2 DKO cells are more sensitive than WT cells to etoposide induced cell death (Fig. S9A). Surprisingly, however, we found that Akt1/2 DKO cells were more resistant than WT cells to cell death induced by increasing concentrations of H_2O_2. The increased sensitivity of WT cells to H_2O_2-mediated cell death was likely due to the activation of Akt and subsequently the phosphorylation and inactivation of FoxO transcription factors, thereby downregulating detoxifying enzymes (Figure 6B). Oxidative stress leads to the activation of Akt either by inactivating PTEN (Leslie et al., 2003) or by the activation of $p66^{shc}$ (Nemoto and Finkel, 2002), or both. In the absence of Akt1 and Akt2, FoxO transcription factors were not significantly inhibited by H_2O_2, thereby maintaining relatively high levels of detoxifying enzymes (Figure 6B). Indeed, expression of DN-FoxO (Fig. S6A) or the knockdown of FoxO3 (Fig. S6B) increased the susceptibility of Akt1/2 DKO MEFs to cell death, whereas expression of activated FoxO in p27-/- MEFs rendered them more resistant to cell H_2O_2 – induced cell death (Figure S6C). Cells expressing activated Akt, or Pten-/- cells, were more susceptible to H_2O_2-induced death (Figure 6C, D). To determine whether scavengers of ROS, regulated by FoxO, are responsible, at least in part, for the resistance of Akt1/2 DKO MEFs to H_2O_2-induced cell death, we knocked down Sesn3 expression in Akt1/2 DKO MEFs or overexpressed catalase in WT MEFs. The knockdown of Sesn3 increased the sensitivity of Akt1/2 DKO MEFs to H_2O_2 (Fig. S6D). Overexpression of catalase decreased the sensitivity of WT MEFs to H_2O_2 (Fig. S6E) but not to the level observed in Akt1/2 DKO MEFs. These results suggest that multiple ROS scavengers induced by FoxO are responsible for the resistance of Akt1/2 DKO MEFs to H_2O_2-induced cell death.

Similar results were obtained when the cells were treated with β-phenylethyl isothiocyanate (PEITC), which is a natural compound found in consumable cruciferous vegetables and is known to increase intracellular ROS levels (Yu et al., 1998). Increasing amounts of PEITC were markedly less effective at killing Akt1/2 DKO cells than WT cells, whereas they were much more effective at killing Pten-/- than Pten+/- cells (Figure S7 A,B). Similar results were observed with other rodent (Figure S7C) or human cells (Figure S7D) expressing activated Akt. We concluded, that, despite the ability of activated Akt to protect against cell death induced by a variety of stimuli, it couldn't protect against ROS–induced cell death. Therefore, because Akt activation increases intracellular ROS levels and impairs ROS scavenging, it not only cannot protect from, but also sensitizes to ROS-induced cell death. Thus, these observations uncovered the Achilles' heel of Akt.

A strategy to selectively eradicate cancer cells with hyperactivated Akt by inducing ROS in combination with rapamycin

Akt is frequently activated in human cancers (reviewed in (Bhaskar and Hay, 2007; Hay, 2005)) and thereby promotes resistance to therapeutic agents that induce apoptosis. Therefore, the hypersensitivity of activated Akt expressing cells to ROS–induced cell death might be exploited to selectively eradicate and to overcome chemoresistance of cancer cells with hyperactivated Akt.

Rapamycin analogs, which are currently used in clinical trials, are mostly cytostatic. One concern in using rapamycin analogs for cancer therapy is that although they may inhibit cell proliferation, they also could increase cell survival via the hyperactivation of Akt due to the inhibition of the negative feedback loop induced by mTORC1 to inhibit Akt activity (reviewed in (Bhaskar and Hay, 2007; Harrington et al., 2005; Hay, 2005)). However, by activating Akt, rapamycin could further sensitize cells to ROS–induced cell death, and thus,

the combination of rapamycin and oxidative stress not only could circumvent resistance to cell death but also would selectively kill cells treated with rapamycin.

To explore this possibility, we first used rodent cells to provide a proof of concept. As shown in Figure S8, rapamycin alone did not induce cell death, but pre-treatment with rapamycin augmented the ability of H_2O_2 to induce apoptosis. Although rapamycin treatment increased H_2O_2-induced apoptosis in both WT and Akt1/2 DKO cells, the level of WT cell apoptosis was significantly higher (Figure S8A). By contrast, rapamycin increased resistance to etoposide (Figs. S9A). Furthermore, activated Akt expressing cells were more sensitive than control cells to cell death induced by the combination of rapamycin and H_2O_2, (Figure S8B), indicating that this cell death is dependent on Akt activity. By contrast, cells expressing activated Akt are more resistant to etoposide, and rapamycin increased this resistance (Fig. S9B). Next we evaluated the effect of rapamycin treatment in combination with PEITC levels that by themselves induce moderate levels of apoptosis (Figure S7). The combination of rapamycin and PEITC significantly increased the moderate levels of apoptosis induced by 3μM and 6μM PEITC, and was even more profound at the selective killing of both rodent and human cells with activated Akt (Fig. S10). Likewise, U251 human glioblastoma cells, deficient in PTEN, were relatively sensitive to PEITC and PEITC plus rapamycin (Fig. 7A and Fig. S11A, B). Re-expression of WT PTEN in these cells rendered them more resistant to PEITC, whereas re-expression of a mutant PTEN maintains their sensitivity (Fig. 7A and Fig. S11A, B). The selective killing of cells with activated Akt was demonstrated by using a mixed population of Rat1a cells in which only about half of the cells co-expressed activated Akt and eGFP. When exposed to PEITC plus rapamycin, most of the dead cells were GFP-positive—clearly demonstrating selective killing (Figure 7B). This is consistent with the further activation of activated Akt by rapamycin (Fig. S12A, B). Notably, rapamycin also increased the susceptibility of cells without hyperactive Akt to killing by PEITC and this is consistent with the ability of rapamycin to activate Akt in these cells (Fig. S12C).

To examine the efficacy of this strategy in cancer cells with hyperactive Akt, we used two ovarian cancer cell lines—TOV21G, in which Akt is hyperactivated even in the absence of serum, and TOV112D in which Akt is not hyperactivated (Figure 7C). In both cell lines rapamycin alone did not induce cell death, whereas PEITC alone induced substantially more TOV21G cell death compared with TOV112D. The combination of PEITC and rapamycin, significantly increased TOV21G cell death and to some extent increased TOV112D cell death (Figure 7C and Fig. S11C, D). This is consistent with the further activation of Akt by rapamycin in TOV21G (Fig. S12B). Furthermore, knockdown of Akt1 and Akt2 in TOV21G cells decreased intracellular levels of ROS (Fig. S13), and markedly decreased their susceptibility to cell death caused by PEITC or PEITC plus rapamycin (Figure 7D). The susceptibility to apoptosis correlated with Akt activity because Akt2 knockdown alone did not significantly decrease total Akt activity, as measured by FOXO phosphorylation (Figure 7D), and also did not decrease susceptibility to apoptosis. However, the knockdown of Akt1 or both Akt1 and Akt2, which markedly decreased Akt activity, also substantially decreased susceptibility to apoptosis induced by PEITC or PEITC plus rapamycin.

TOV21G cells were significantly more resistant to etoposide-induced apoptosis than TOV112D cells (Fig. S14A). However, expression of activated Akt in TOV112D cells rendered them more resistant to etoposide but more sensitive to PEITC (Fig. S14B, C). While rapamycin increased sensitivity to PEITC, it decreased sensitivity to etoposide (Fig. S14A, B). We concluded that PEITC could be used to selectively kill cells expressing hyperactive Akt or cells treated with rapamycin due to the ability of rapamycin to activate Akt.

To verify the in vitro results, in vivo, we employed xenografts of cancer cells in athymic mice. We first determined tumor growth of TOV112D and TOV112D (mAkt) cells. As shown in Fig. 8A, the growth of TOV112D tumors were relatively sensitive to etoposide when compared with TOV112D (mAkt) tumors, which display almost a complete resistance to etoposide. By contrast, TOV112D (mAkt) tumors were markedly more sensitive to PEITC than TOV112D cells. We then studied the effect of PEITC and rapamycin on the growth of tumors induced by TOV21G cells (Fig. 8B). Rapamycin or PEITC alone moderately attenuated the growth of the tumors. However, the combination of PEITC and rapamycin regressed tumor growth and eradicated the tumors. Analyses of tumor sections, at the endpoint of the experiment, showed that PEITC alone induced a profound cells death as assessed by cleaved caspase 3, whereas rapamycin alone that elicited an increase in Akt activation, did not induce cell death but markedly inhibited BrdU incorporation (Fig. 8C,D). At the endpoint of the experiment no tumors were found after treatment with both PEITC and rapamycin, and therefore tumor sections were not analyzed. We, therefore, analyzed tumor sections 28 days after inoculation of the cells, and it was evident that cell death, as measured by cleaved caspase 3, was profoundly higher after administration of both PEITC and rapamycin than after administration of PEITC alone (Fig. 8D). Thus, these results recapitulate our in vitro observations, in vivo, and reinforce the notion that rapamycin alone is mostly cytostatic, while PEITC inhibits tumor growth by eliciting cell death, overriding the resistance to cell death mediated by activated Akt. In these studies, we could not compare TOV21G to TOV21G cells in which Akt genes were knocked down because the later could not form tumors within the time frame of the experiment. Collectively, these results provide a proof of concept, in vivo, that cell death induced by oxidative stress can selectively attenuate growth of tumor cells with hyperactivated Akt, and that the combination of oxidative stress and rapamycin could be an effective strategy to selectively eradicate tumors that display hyperactive Akt.

Discussion

We show here that Akt-deficiency inhibits replicative and premature senescence induced by oxidative stress and activated Ras, whereas Akt activation induces premature senescence. The effect of Akt on cellular senescence is mediated by intracellular ROS. Akt elevates ROS levels by two mechanisms. First, the increase in oxygen consumption by Akt also increases ROS generation. Second, Akt impairs ROS scavenging by inhibiting FoxOs transcription factors. FoxOs decrease ROS and inhibit cellular senescence, while the deficiency of FoxOs increase ROS and cellular senescence. The role of Akt and FoxO in cellular senescence could be extended to human cells because although telomerase activity is a major determinant of human cell lifespan, oxygen consumption as well appears to play a role in their lifespan in culture (Packer and Fuehr, 1977). Indeed, we showed that HDFs deficient in Akt have an extended lifespan in culture and are more resistant to oxidative stress induced senescence. Therefore, at least at the cellular level, the role of Akt and FoxO in regulating lifespan is conserved in mammals. Moreover, in addition to known ROS scavengers regulated by FoxOs, we found that FoxO1 elevates the expression of Sesn3 that was shown to reduce intracellular ROS levels by regenerating overoxidized peroxiredoxins that deoxidize ROS (Budanov et al., 2004). Consistently Sesn3 levels are elevated in Akt1/2 DKO MEFs, and the reduction of Sesn3 levels in these cells increases intracellular ROS level to a level similar to that observed in WT cells (Fig. 3, G-J). These results suggest that Sesn3 is a major determinant of ROS levels regulated by FoxO and Akt.

A similar paradigm exists in response to lethal doses of oxidants. While Akt-deficiency inhibits, Akt activation accelerates cell death induced by ROS, and the activation of FoxO inhibits this cell death. These results are consistent with the observation that hematopoietic stem cells in FoxO-deficient mice are sensitive to oxidative stress (Tothova et al., 2007).

Although ROS can also induce necrotic cell death, we found that under our conditions most of the cells died by apoptosis as assessed by nuclear condensation and fragmentation. The mechanisms by which activated Akt induces ROS, which in turn sensitize cells to either senescence or apoptosis are summarized schematically in Figure 8E.

The role of Akt in energy metabolism—pro-and anti-cancer

The effect of Akt on tumorigenesis could be mediated through its effect on energy metabolism (Robey and Hay, 2006). Here we showed that Akt activation increases ROS levels, partially via its role in energy metabolism. The increase in ROS levels mediated by Akt could contribute to tumorigenisis by increasing mutation rate and genetic instability. However, at the same time this also could be a barrier to tumorigenesis because an increase in intracellular ROS levels mediated by Akt render cells more susceptible to premature senescence unless they acquired an immortalizing mutation such as p53 dysfunction. Cells in which PTEN is deleted are also more susceptible to premature senescence, and therefore the deletion of p53 markedly increases tumorigenesis mediated by the deletion of PTEN (Chen et al., 2005). Our results suggest that the senescence induced by PTEN deletion is likely due to the activation of Akt and the increase in intracellular ROS.

Because elevated levels of ROS increases Akt activity (Figure 6B), it is possible that Akt would induce a vicious cycle of further and sustained Akt activation concomitant with a sustained increase in intracellular ROS level, and therefore a sustained increase in a mutation rate. If cells escape the barrier of senescence, this could be a major contributing factor for tumorigenicity induced by Akt activation. However, here again this contribution of Akt to tumorigenesis is also the Achilles' heel of Akt. Despite the ability of activated Akt to inhibit apoptosis induced by a variety of apoptotic stimuli it cannot protect against lethal doses of ROS, and this could be exploited for cancer therapy.

It was previously shown that oxidative stress can induce selective killing of cells expressing Bcr-Abl or activated Ras (Trachootham et al., 2006). However, because of the anti-apoptotic activity of Akt, it could not be predicted that activation of Akt also sensitizes cells to oxidative stress–induced cell death. In fact, our results suggest that Akt activation by Ras is likely the reason why cells expressing activated Ras are sensitized to killing by oxidative stress. This might also apply to Bcr-Abl because Bcr-Abl also can activate Akt (Skorski et al., 1997).

Future implications: A strategy that selectively eradicates cancer cells with activated Akt

Akt is perhaps the most frequently activated oncoprotein in human cancers. Akt is activated by multiple mechanisms including, Pten mutations, p110 activating mutations, Ras activation, and receptor tyrosine kinases activation (reviewed in (Bhaskar and Hay, 2007; Hay, 2005). Thus, Akt is an attractive target for cancer therapy. Although we have previously provided a proof of concept that partial ablation of Akt or the deletion of Akt1 is sufficient to impede tumor development without having other severe physiological consequences, (Chen et al., 2006; Ju et al., 2007; Skeen et al., 2006) there is still a concern that ablation of Akt might lead to undesired physiological consequences such as diabetes. Thus, a strategy to selectively eradicate cancer cells with hyperactivated Akt is highly desirable. Our observation that cancer cells expressing activated Akt are selectively killed by oxidative stress circumvents this concern. Furthermore, our results show that rapamycin treatment, which by itself is only cytostatic, also increases Akt activity, which in turn increases resistance to etoposide but further sensitizes cells to oxidative stress–induced apoptosis.

We provided a proof of concept for this strategy, in vivo, in xenografts model by showing that the combination of the ROS-inducer, PEITC, and rapamycin could completely eradicate the growth of tumors in which Akt is hyperactivated. Furthermore, we showed that tumors expressing activated Akt are more resistant to etoposide but more sensitive to PEITC than tumors that do not express activated Akt. We did not intend to provide the exact regimen for this strategy but we found that, at least at the cellular level the ROS-inducer, 2-methoxyestradiol (2-ME) (Hileman et al., 2004), which is currently used in clinical trials is also effective in the selective killing of cells with hyperactivated Akt (Fig. S15). Thus, this strategy not only could eliminate the concern that rapamycin treatment activates Akt but also would take advantage of this phenomenon to selectively eradicate rapamycin-treated cancer cells. The combination of rapamycin and oxidative stress could be an attractive general strategy for cancer therapy not necessarily only for cancer cells with hyperactivated Akt, particularly since rapamycin analogs are already being used in advanced stages of clinical trials.

Experimental procedures

Cells and viruses

Primary MEFs were harvested from E13.5 embryos as previously described (Skeen et al., 2006). Experiments using primary cells were performed no later than passage 3. Experiments were also performed on wild type, Akt1/2$^{-/-}$, FoxO3$^{+/+}$ and FoxO3$^{-/-}$ MEFs immortalized by DN-p53 as previously described (Skeen et al., 2006). Other cell lines used are: Pten$^{+/-}$p53$^{-/-}$, Pten$^{-/-}$p53$^{-/-}$ MEFs, Rat1a, HEK293, the glioblastoma cell line, U251, and the ovarian cancer cells lines (TOV112D, TOV21G). Cells were maintained in DMEM supplemented with 10% FBS. TOV112D and TOV21G cells were grown in M199/MCDB medium (1:1) with 15% FBS.

Retroviruses and lentiviruses infection and generation, and knockdown procedures are described in Supplemental Material.

Population doubling

Serial 3T3 cultivation was carried out as described previously (Pantoja and Serrano, 1999). Briefly, cells (2×10^5/60 mm plate) were grown for 3 or 5 days. Cells were split every 3 or 5 days and replated at the same density (2×10^5). This procedure was repeated for 20 passages. The increase in population doubling level (PDL) was calculated by the formula PDL=log (n_f/n_0)/log 2, where n_0 is the initial number of cells and n_f is the final number of cells. Data were expressed as cumulated PDL from three independent experiments using three pairs of MEFs.

Senescence associated β-galactosidase (SA-β-gal) staining

Cells were plated at low density (8000 cells/35-mm plate), fixed, and stained for SA-β-Gal as described in (Dimri et al., 1995; Serrano et al., 1997) at different time points as indicated.

BrdU labeling

To determine actively replicating cells, BrdU incorporation assays were performed as described in (Skeen et al., 2006).

Oxygen consumption assay

For oxygen consumption measurement, cells were grown overnight. Cells were then harvested, washed with PBS and resuspended in 500 μl of fresh DMEM. The rate of oxygen consumption was measured at 37°C using a Strathkelvin Model 782 oxygen meter equipped

with a Clark-type oxygen electrode. Results are expressed as nanomoles of oxygen consumed per minute and per million cells.

Measurement of ROS

Intracellular ROS generation was assessed using 2', 7'-dichlorofluorescein diacetate (Molecular Probes). For details see Supplemental Material.

Western blot analysis

For western blot analysis, 10^6 cells were plated in 10-cm plates and grown overnight. The whole cell extract were prepared in lysis buffer as described (Hahn-Windgassen et al., 2005).

Real-time PCR and primers

See Supplemental Material.

Hydrogen peroxide-induced senescence

Primary MEFs plated at 40% confluency were treated for 2 h with 75 μM H_2O_2 in DMEM containing 10% FCS (day –9). Cells were then washed, incubated in fresh medium for 7 days and treated a second time for 2 h with 75 μM H_2O_2 (day –2). Cells were then washed, incubated in fresh medium for 48 h, and subcultured at low confluency (day 0) for up to 17 days. At days 3, 10, and 17, cells were checked for SA β-galactosidase activity, BrdU incorporation, ROS production and cell lysates were prepared for western blotting.

Ras-induced senescence

Primary MEFs (1.5×10^5/60 mm plate) were infected with pBabe-Hygro or pBabe-Hygro-H-Ras^{valine12} retroviruses and selected with 150-μg/ml hygromycin for 36 h. At the end of the selection, cells were grown for 48 h and subcultured for experiments (day 0).

Activated Akt-induced senescence

Primary MEFs (1.5×10^5/60mm plate) were infected with pBabePuro-mAkt-ER retrovirus and were selected with 2μg/ml puromycin for 72h. At the end of the selection, cells were allowed to grow for 48h and subcultured for experiments (day 0). To induce mAkt activity, cells were incubated with 300nM 4-Hydroxytamoxifen (4-OHT) for 48h.

Apoptosis assays

Cells were plated at 40% confluence, allowed to grow overnight, and then subjected to the following treatments: (i) increasing concentrations of H_2O_2 (100 μM to 1 mM) in DMEM for 2h; (ii) exposure to 100 nM rapamycin for 3h prior to the addition of H_2O_2, (iii) exposure to PEITC as described in figure legends; (iv) exposure to 100 nM rapamycin for 3h prior to the addition of PEITC. To quantify apoptosis, cells were then fixed for DAPI staining as previously described (Kennedy et al., 1999). The PEITC/rapamycin-induced apoptosis in Rat1a-mAktGFP cells is described in Supplemental Material.

Xenografts studies

Male athymic mice (6-8 weeks old) were purchased from Charles River Laboratories. Cells (TOV21G, TOV112D, and TOV112D (mAkt), 2×10^6/0.1 ml PBS) were injected subcutaneously on both left and right flanks of each mouse. Mice were equally randomized into different groups of treatment (see Figure Legend). When tumor reached a size of 10 to 15 mm^3, animals were treated with indicated drugs, PEITC (35 mg/kg), Rapamycin (2 mg/kg), Etoposide (10mg/kg) and combination of Rapamycin/PEITC (1:1) or Rapamycin/

Etoposide (1:1) from Monday to Friday by intraperitoneal injection. For more details see Supplementary Material. All animal experiments were in accordance with the animal care policies of the University of Illinois at Chicago and were approved by the animal care committee of the University of Illinois at Chicago.

Histopathology and immunohistochemistry

Tumors were collected at indicated time points, rinsed in PBS, and fixed in 4% paraformaldehyde overnight. Following the fixation, fixed tissues were processed and embedded in paraffin. Immunohistochemistry assays were preformed as described in (Chen et al., 2006). The primary antibodies included anti-cleaved caspase-3 (Asp175) and anti-phospho Akt (ser473) (Cell Signaling). Biotin-conjugated secondary antibody kits, avidin–biotin complexes, and diaminobenzidine were purchased from Vector Laboratories. For quantification, cells were counted from four fields at 400**x** magnifications.

BrdU incorporation assay in mice

BrdU incorporation assays were performed as in (Chen et al., 2006). Briefly, mice were given i.p. injections of 0.5 mg of BrdU per 10 g of body weight for 2h prior to sacrifice.

Supplementary Material

Refer to Web version on PubMed Central for supplementary material.

Acknowledgments

We would like to thank Beatrice Knudsen (Fred Hutchinson Cancer Research Center) for the TOV-112D and TOV-21G cell lines and for sharing unpublished information. We would also like to thank Yongmei Luo for technical assistance and Prashanth Bhaskar, and Deepa Sunararajan for discussion, comments on the manuscript, and reagents. We also thank Navdeep Chandel for advice. These studies were supported by NIH grants CA090764, AG016927, and AG025953 to N.H., and by ACS-IL 06-24 to Y.P.

References

Balaban RS, Nemoto S, Finkel T. Mitochondria, oxidants, and aging. Cell 2005;120:483–495. [PubMed: 15734681]

Bhaskar PT, Hay N. The Two TORCs and Akt. Dev Cell 2007;12:487–502. [PubMed: 17419990]

Braig M, Lee S, Loddenkemper C, Rudolph C, Peters AH, Schlegelberger B, Stein H, Dorken B, Jenuwein T, Schmitt CA. Oncogene-induced senescence as an initial barrier in lymphoma development. Nature 2005;436:660–665. [PubMed: 16079837]

Budanov AV, Sablina AA, Feinstein E, Koonin EV, Chumakov PM. Regeneration of peroxiredoxins by p53-regulated sestrins, homologs of bacterial AhpD. Science 2004;304:596–600. [PubMed: 15105503]

Budanov AV, Shoshani T, Faerman A, Zelin E, Kamer I, Kalinski H, Gorodin S, Fishman A, Chajut A, Einat P, et al. Identification of a novel stress-responsive gene Hi95 involved in regulation of cell viability. Oncogene 2002;21:6017–6031. [PubMed: 12203114]

Chance B, Sies H, Boveris A. Hydroperoxide metabolism in mammalian organs. Physiol Rev 1979;59:527–605. [PubMed: 37532]

Chen ML, Xu PZ, Peng X, Chen WS, Guzman G, Yang X, Di Cristofano A, Pandolfi PP, Hay N. The deficiency of Akt1 is sufficient to suppress tumor development in Pten+/- mice. Genes Dev 2006;20:1569–1574. [PubMed: 16778075]

Chen Z, Trotman LC, Shaffer D, Lin HK, Dotan ZA, Niki M, Koutcher JA, Scher HI, Ludwig T, Gerald W, et al. Crucial role of p53-dependent cellular senescence in suppression of Pten-deficient tumorigenesis. Nature 2005;436:725–730. [PubMed: 16079851]

Gottlob K, Majewski N, Kennedy S, Kandel E, Robey RB, Hay N. Inhibition of early apoptotic events by Akt/PKB is dependent on the first committed step of glycolysis and mitochondrial hexokinase. Genes Dev 2001;15:1406–1418. [PubMed: 11390360]

Greer EL, Brunet A. FOXO transcription factors at the interface between longevity and tumor suppression. Oncogene 2005;24:7410–7425. [PubMed: 16288288]

Hahn-Windgassen A, Nogueira V, Chen CC, Skeen JE, Sonenberg N, Hay N. Akt activates the mammalian target of rapamycin by regulating cellular ATP level and AMPK activity. J Biol Chem 2005;280:32081–32089. [PubMed: 16027121]

Harrington LS, Findlay GM, Lamb RF. Restraining PI3K: mTOR signalling goes back to the membrane. Trends Biochem Sci 2005;30:35–42. [PubMed: 15653324]

Hay N. The Akt-mTOR tango and its relevance to cancer. Cancer Cell 2005;8:179–183. [PubMed: 16169463]

Hileman EO, Liu J, Albitar M, Keating MJ, Huang P. Intrinsic oxidative stress in cancer cells: a biochemical basis for therapeutic selectivity. Cancer Chemother Pharmacol 2004;53:209–219. [PubMed: 14610616]

Ju X, Katiyar S, Wang C, Liu M, Jiao X, Li S, Zhou J, Turner J, Lisanti MP, Russell RG, et al. Akt1 governs breast cancer progression in vivo. Proc Natl Acad Sci U S A 2007;104:7438–7443. [PubMed: 17460049]

Kandel ES, Skeen J, Majewski N, Di Cristofano A, Pandolfi PP, Feliciano CS, Gartel A, Hay N. Activation of Akt/protein kinase B overcomes a G(2)/m cell cycle checkpoint induced by DNA damage. Mol Cell Biol 2002;22:7831–7841. [PubMed: 12391152]

Kennedy SG, Kandel ES, Cross TK, Hay N. Akt/Protein kinase B inhibits cell death by preventing the release of cytochrome c from mitochondria. Mol Cell Biol 1999;19:5800–5810. [PubMed: 10409766]

Kopnin PB, Agapova LS, Kopnin BP, Chumakov PM. Repression of sestrin family genes contributes to oncogenic Ras-induced reactive oxygen species up-regulation and genetic instability. Cancer Res 2007;67:4671–4678. [PubMed: 17510393]

Kops GJ, Dansen TB, Polderman PE, Saarloos I, Wirtz KW, Coffer PJ, Huang TT, Bos JL, Medema RH, Burgering BM. Forkhead transcription factor FOXO3a protects quiescent cells from oxidative stress. Nature 2002;419:316–321. [PubMed: 12239572]

Lee AC, Fenster BE, Ito H, Takeda K, Bae NS, Hirai T, Yu ZX, Ferrans VJ, Howard BH, Finkel T. Ras proteins induce senescence by altering the intracellular levels of reactive oxygen species. J Biol Chem 1999;274:7936–7940. [PubMed: 10075689]

Leslie NR, Bennett D, Lindsay YE, Stewart H, Gray A, Downes CP. Redox regulation of PI 3-kinase signalling via inactivation of PTEN. Embo J 2003;22:5501–5510. [PubMed: 14532122]

Matheu A, Maraver A, Klatt P, Flores I, Garcia-Cao I, Borras C, Flores JM, Vina J, Blasco MA, Serrano M. Delayed ageing through damage protection by the Arf/p53 pathway. Nature 2007;448:375–379. [PubMed: 17637672]

Nemoto S, Finkel T. Redox regulation of forkhead proteins through a p66shc-dependent signaling pathway. Science 2002;295:2450–2452. [PubMed: 11884717]

Packer L, Fuehr K. Low oxygen concentration extends the lifespan of cultured human diploid cells. Nature 1977;267:423–425. [PubMed: 876356]

Palmero I, Pantoja C, Serrano M. p19ARF links the tumour suppressor p53 to Ras. Nature 1998;395:125–126. [PubMed: 9744268]

Parrinello S, Samper E, Krtolica A, Goldstein J, Melov S, Campisi J. Oxygen sensitivity severely limits the replicative lifespan of murine fibroblasts. Nat Cell Biol 2003;5:741–747. [PubMed: 12855956]

Plas DR, Thompson CB. Akt-dependent transformation: there is more to growth than just surviving. Oncogene 2005;24:7435–7442. [PubMed: 16288290]

Robey RB, Hay N. Mitochondrial hexokinases, novel mediators of the antiapoptotic effects of growth factors and Akt. Oncogene 2006;25:4683–4696. [PubMed: 16892082]

Rossignol R, Gilkerson R, Aggeler R, Yamagata K, Remington SJ, Capaldi RA. Energy substrate modulates mitochondrial structure and oxidative capacity in cancer cells. Cancer Res 2004;64:985–993. [PubMed: 14871829]

Sablina AA, Budanov AV, Ilyinskaya GV, Agapova LS, Kravchenko JE, Chumakov PM. The antioxidant function of the p53 tumor suppressor. Nat Med 2005;11:1306–1313. [PubMed: 16286925]

Schmitt CA. Cellular senescence and cancer treatment. Biochim Biophys Acta 2007;1775:5–20. [PubMed: 17027159]

Serrano M, Lin AW, McCurrach ME, Beach D, Lowe SW. Oncogenic ras provokes premature cell senescence associated with accumulation of p53 and p16INK4a. Cell 1997;88:593–602. [PubMed: 9054499]

Skeen JE, Bhaskar PT, Chen CC, Chen WS, Peng XD, Nogueira V, Hahn-Windgassen A, Kiyokawa H, Hay N. Akt deficiency impairs normal cell proliferation and suppresses oncogenesis in a p53-independent and mTORC1-dependent manner. Cancer Cell 2006;10:269–280. [PubMed: 17045205]

Skorski T, Bellacosa A, Nieborowska-Skorska M, Majewski M, Martinez R, Choi JK, Trotta R, Wlodarski P, Perrotti D, Chan TO, et al. Transformation of hematopoietic cells by BCR/ABL requires activation of a PI-3k/Akt-dependent pathway. Embo J 1997;16:6151–6161. [PubMed: 9321394]

Tothova Z, Kollipara R, Huntly BJ, Lee BH, Castrillon DH, Cullen DE, McDowell EP, Lazo-Kallanian S, Williams IR, Sears C, et al. FoxOs are critical mediators of hematopoietic stem cell resistance to physiologic oxidative stress. Cell 2007;128:325–339. [PubMed: 17254970]

Trachootham D, Zhou Y, Zhang H, Demizu Y, Chen Z, Pelicano H, Chiao PJ, Achanta G, Arlinghaus RB, Liu J, Huang P. Selective killing of oncogenically transformed cells through a ROS-mediated mechanism by beta-phenylethyl isothiocyanate. Cancer Cell 2006;10:241–252. [PubMed: 16959615]

Warburg O, Geissler AW, Lorenz S. [On growth of cancer cells in media in which glucose is replaced by galactose]. Hoppe Seylers Z Physiol Chem 1967;348:1686–1687. [PubMed: 5586915]

Yu R, Mandlekar S, Harvey KJ, Ucker DS, Kong AN. Chemopreventive isothiocyanates induce apoptosis and caspase-3-like protease activity. Cancer Res 1998;58:402–408. [PubMed: 9458080]

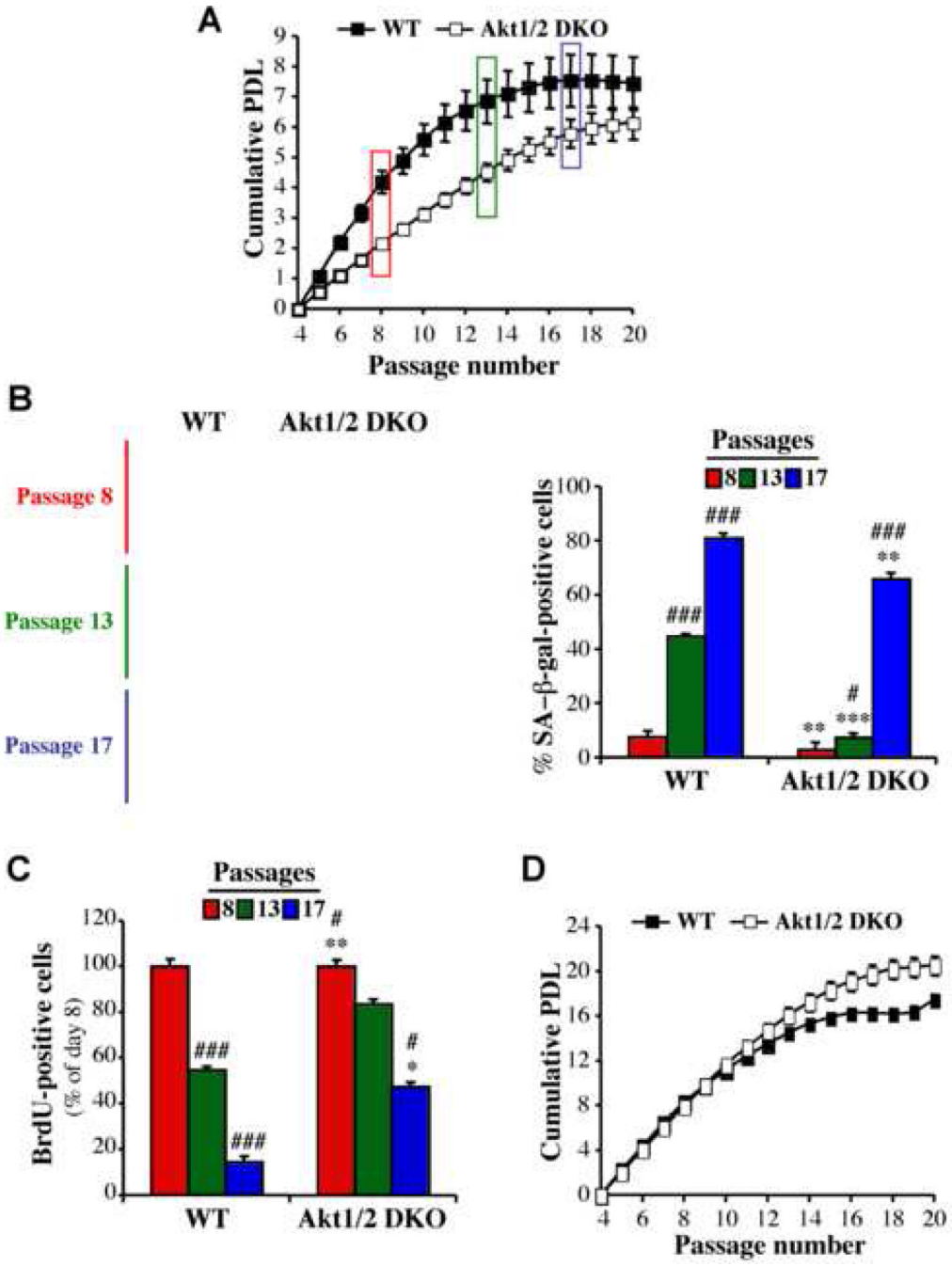

Figure 1. Akt regulates replicative senescence

A. Cells were subjected to the 3T3 protocol as described in Experimental Procedures. Cells were counted at each passage every 3 days, and the population doubling (PDL) was calculated for wild-type (WT) and Akt1/2 null (Akt1/2 DKO) primary MEFs. **B**. Primary MEFs were stained for SA-β-gal activity at passage 8 (before visible signs of senescence), at passage 13 when WT cells began to exhibit proliferative arrest, and at passage 17 when Akt1/2 DKO cells began to exhibit proliferative arrest. Left Panels: representative photographic images of cells stained for SA-β-gal activity at passage number 8, 13 and 17. Right panel: SA-β-gal-positive cells were counted in at least 5 fields of triplicate plates. Data represent the mean ± S.E.M. of three independent experiments. *, **, $p<0.05$, 0.01 vs. WT.

#, ###, p<0.05, 0.001 vs. Passage 8. **C**. Proliferation rate of primary MEFs as measured by BrdU labeling for 24 hr prior to fixation and staining. BrdU incorporation was carried out as described in the Experimental Procedures and determined by counting at least 150 cells from at least 5 fields in triplicate plates. Data represent the mean ± S.E.M. of three independent experiments. *,**, *** p<0.05, 0.01, 0.001 vs. WT. #, ###, p<0.05, 0.001 vs. Passage 8. **D.** Cumulative PDL of WT and Akt1/2 DKO primary MEFs as described in (A) except that cells were split and counted every 5 days. Data represent the mean ± S.E.M. of at least three independent experiments.

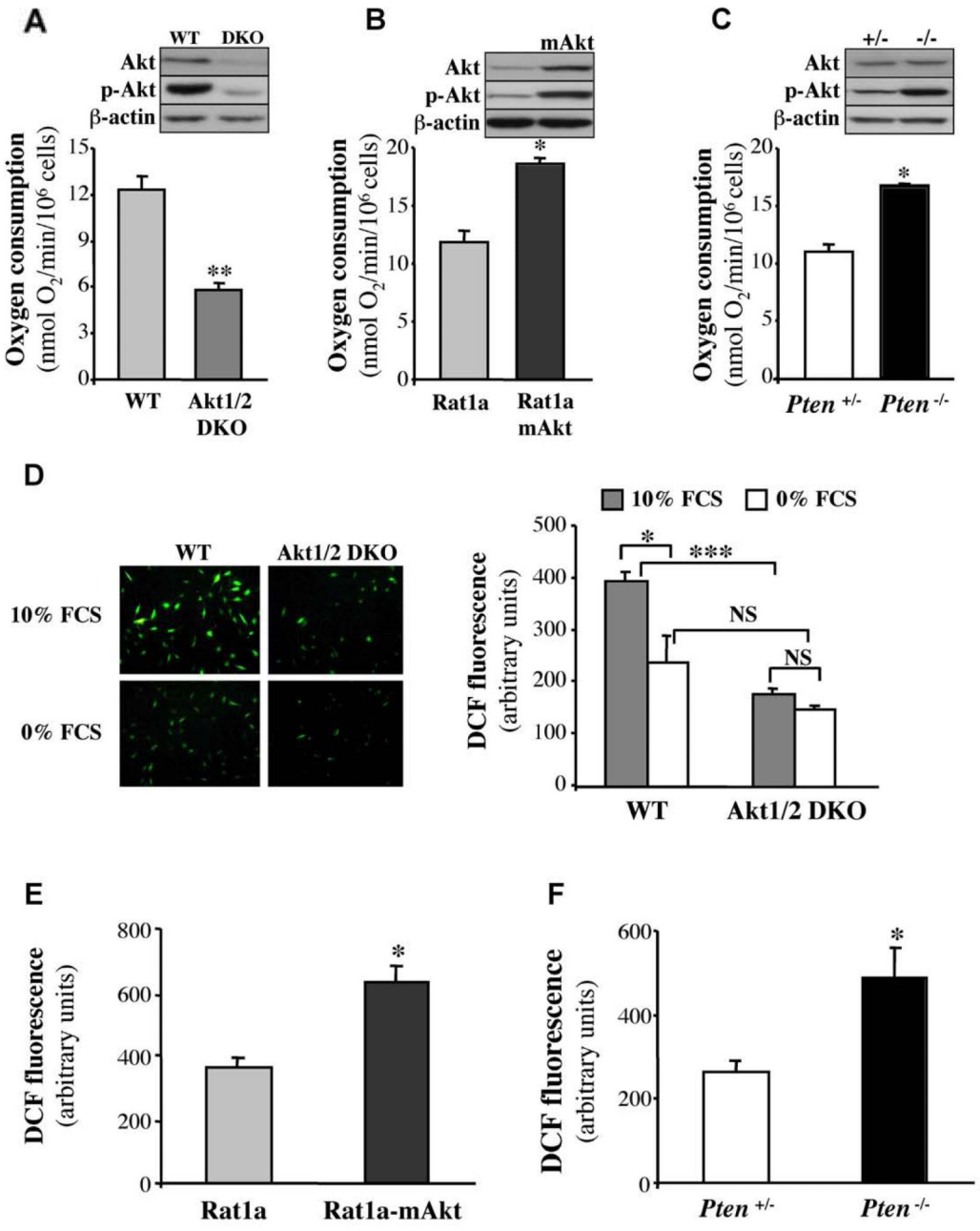

Figure 2. Akt regulates oxygen consumption and ROS generation

A-C. Rates of oxygen consumption in WT or Akt1/2 DKO MEFs (A), Rat1a, or Rat1a expressing activated Akt (Rat1a mAkt) (B), and Pten$^{+/-}$ or Pten$^{-/-}$ MEFs (C) were measured as described in Experimental Procedures. Immunoblots show the relative level of phosphorylated Akt (p-Akt Ser 473) and total Akt in all cell lines. Data represent the mean ± S.E.M. of at least three independent experiments. *, ** $p<0.05$, 0.01 vs. WT (A), Rat1a (B) and PTEN$^{+/-}$ (C). **D-F.** Akt mediates the generation of ROS. D. Levels of ROS in WT and Akt1/2 DKO MEFs incubated in 10% FBS or in 0% FBS overnight. Left panels: representative images of cells stained with DCF. Right panel: quantification of ROS levels. *, $P < 0.05$; ***, $P < 0.001$; NS, not significant. E. Levels of ROS in Rat1a and Rat1a-mAkt cells. F. Level of ROS in Pten$^{+/-}$ and Pten$^{-/-}$ MEFs. Data are expressed as arbitrary units

after being normalized to protein concentration. All data represent the mean ± S.E.M. of at least three independent experiments. *, $p<0.05$ vs. Rat1a (E) or $Pten^{+/-}$ (F).

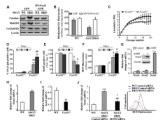

Figure 3. FoxO transcription factors regulate the generation of ROS and replicative senescence downstream of Akt

A. Catalase and MnSOD are upregulated in Akt1/2 DKO MEFs, and are downregulated by DN-FoxO. The generation of cells expressing DN-FOXO is described in Experimental Procedures. Proteins extracted from exponentially growing DNp53-immortalized WT and Akt1/2 DKO MEFs overexpressing GFP (control vector) or DN-FOXO-GFP were subjected to immunoblotting using antibodies specific for catalase, MnSOD, Cu/ZnSOD and β actin as a loading control. **B.** DN-FOXO restores intracellular level of ROS in Akt1/2 DKO cells. Quantification of ROS in WT and Akt1/2 DKO MEFs overexpressing GFP or DN-FOXO-GFP after incubation of cells with rhodamine123 as a sensor of ROS production (described in Experimental Procedures). Data represent the mean ± S.E.M. of three independent experiments. *, $p<0.05$ vs. GFP-WT. #, $p<0.05$ vs. GFPAkt1/2 DKO. **C.** Wild-type ($FOXO3^{+/+}$) and FOXO3 null ($FOXO3^{-/-}$) primary MEFs were analyzed for replicative senescence using the 3T3 protocol. Cumulative PDL is plotted against Passage Number. Data represent the mean ± S.E.M. of three independent experiments. **D.** SA-β-gal activity in primary $FOXO3^{+/+}$ and $FOXO3^{-/-}$ cells. Assay was performed at 3, 10 and 17 days in culture. *, **, $p<0.05$, 0.01 vs. $FOXO3^{+/+}$, ##, $p<0.01$ vs. Day 3. **E.** Cell proliferation was assessed by BrdU incorporation at the same time points shown in (D). *, $p<0.05$ vs. $FOXO3^{+/+}$, #, $p<0.05$ vs. Day 3. Data represent the mean ± S.E.M. of three independent experiments. **F.** Level of ROS in primary $FOXO3^{+/+}$ and $FOXO3^{-/-}$ cells at the same time points as in (D). Data are presented as arbitrary units after being normalized to protein concentration. *, **, $p<0.05$, 0.01 vs. $FOXO3^{+/+}$, #, $p<0.05$ vs. Day 3. Data represent the mean ± S.E.M. of at least three independent experiments. **G.** Left panel. Level of Sestrin 1, 2 and 3 mRNA as determined by quantitative RT-PCR. Wild type MEFs immortalized with DN-p53 and stably expressing FoxO1AAA-ER were treated with 4-OHT followed by RNA analysis as described in Experimental Procedures. ***, $p<0.001$ vs. control. Right panel. Immunoblot showing induction of Sesn3 protein level after FoxO1AAA-ER activation by 4-OHT. **H.** Level of Sestrin 3 mRNA in WT and Akt1/2 DKO MEFs, immortalized with DN-p53, as assessed by quantitative RT-PCR. **, $p<0.01$ vs. WT. **I.** Level of Sestrin 3 mRNA in WT and $FOXO3^{-/-}$ MEFs immortalized with DN-p53. All RNA analyses were done in triplicates. **, $p<0.001$ vs. WT. **J.** The knockdown of Sesn3 in Akt1/2 DKO MEFs elevates ROS levels to that in WT cells. Left panel: Levels of Sesn3 mRNA in WT, Akt1/2 DKO and Akt1/2 DKO-Sesn3 KD MEFs as assessed by quantitative RT-PCR. *, ***, $p<0.05$, 0.001 vs. control siRNA in WT and ##, $p<0.01$ vs. control siRNA in Akt1/2 DKO. Data represent the mean ± S.E.M. of three independent experiments. Right panel: Levels of ROS in WT, Akt1/2 DKO and Akt1/2 DKO-SESN3 KD MEFs as assessed by DCF fluorescence.

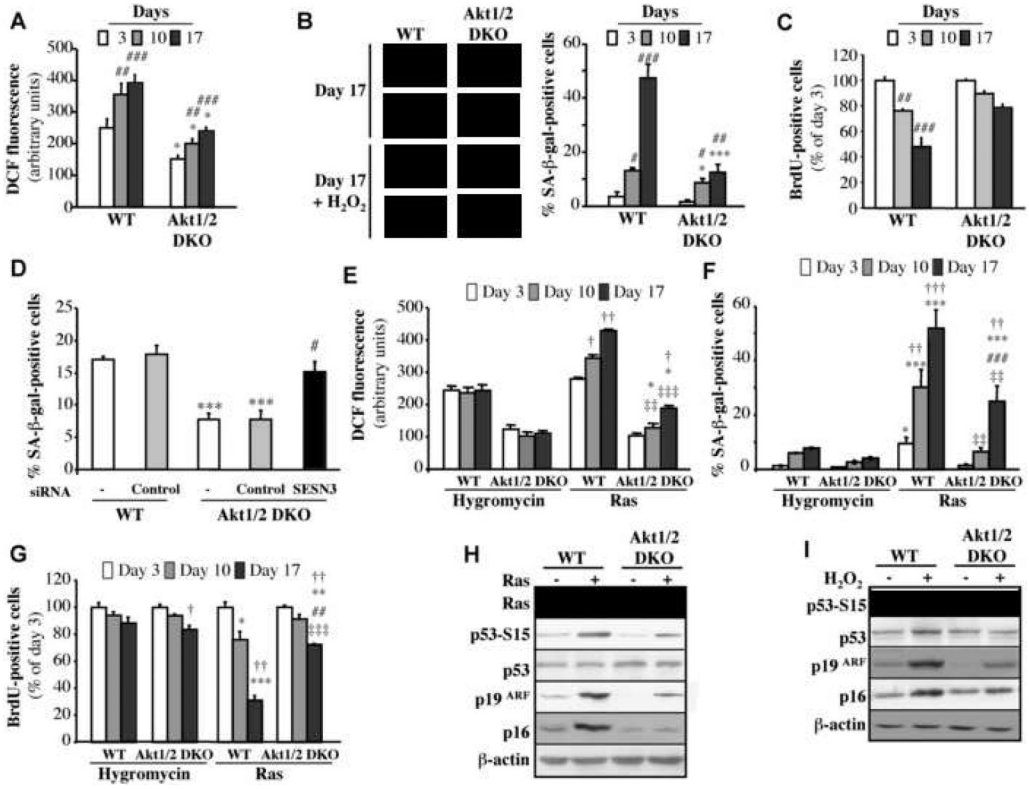

Figure 4. Akt deficiency exerts resistance to H_2O_2- and Ras-induced premature senescence

Premature senescence of primary WT and Akt1/2 DKO MEFs was induced with 75 μM H_2O_2 as described in Experimental Procedures. At days 3, 10 and 17 after treatment cells were analyzed for: **A.** ROS production **B.** SA-β-gal activity (Left Panels: representative images of cells stained for F-actin/DAPI (fluorescence) and SA-β-gal activity (brightfield) at Day 17. Right panel: β-gal-positive cells. **C.** BrdU incorporation. *, ***, p<0.05, 0.001 vs. WT and ##, ###, p<0.01, 0.001 vs. Day 3. **D.** The knockdown of Sesn3 overrides the resistance of Akt1/2 DKO MEFs to H_2O_2-induced senescence. Premature senescence of primary WT and Akt1/2 DKO MEFs was induced with 75 μM H_2O_2 as described in Experimental Procedures, and at day 0, cells were transfected with siRNAs and then cells were analyzed for SA-β-gal activity at day 7 post transfection. *** p<0.001 vs. WT; # p<0.05 vs. Akt1/2 DKO.

E-G. Primary WT and Akt1/2 DKO MEFs were infected with empty vector (Hygromycin) or H-Ras^{val12}-expressing retroviruses. At days 3, 10 and 17 post selection (see Experimental Procedures), the cells were analyzed for: **E**, ROS production; **F**, SA-β-gal activity; and **G**, BrdU incorporation. *, **, *** p<0.05, 0.01, 0.001 vs. WT-Hygro; ##, ### p<0.01, 0.001 vs. Akt1/2 DKO-Hygro; ‡‡, ‡‡‡ p<0.01, 0.001 vs. WT-Ras; †, ††, ††† p<0.05, 0.01, 0.001 vs. Day 3. **H.** Immunoblot showing expression of Ras, showing p53 phospho-Ser15, total p53, p19^{ARF}, and p16 following expression of H-Ras^{v12} in wild-type or Akt1/2 DKO MEFs. **I.** Immunoblot showing p53 phospho-Ser15, total p53, p19^{ARF}, and p16 following addition of H_2O_2 to wild-type or Akt1/2 DKO MEFs. All data represent the mean ± S.E.M. of at least three independent experiments.

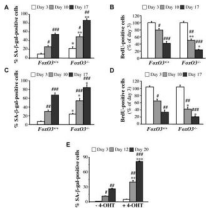

Figure 5. FoxO3-/- MEFs are sensitized to H_2O_2 and Ras induced premature senescence (A-D). Primary $FoxO3^{+/+}$ and $FoxO3^{-/-}$ MEFs were treated with 75μM H_2O_2. At days 3, 10 and 17-post treatment, cells were analyzed for: **A**, SA-β-gal activity; and **B**, BrdU incorporation. Primary $FoxO3^{+/+}$ and $FoxO3^{-/-}$ MEFs were infected with retrovirus expressing $H\text{-}Ras^{v12}$. At days 3, 10 and 17 post selection, cells were analyzed for: **C**, SA-β-gal activity; and **D**, BrdU incorporation. All data represent the mean ± S.E.M. of at least three independent experiments. *,** p<0.05, 0.01 vs. $FOXO3^{+/+}$; #, ##, ### p<0.05, 0.01, 0.001 vs. Day 3. E. Activated Akt induces premature senescence of MEFs. Primary wild-type MEFs were infected with retrovirus expressing inducible myristoylated Akt (mAkt-ER). After selection, cells were either untreated or treated with 4-OHT. At days 3, 12 and 20-post incubation with 4-OHT, cells were analyzed for SA-β-gal activity. Data represent the mean ± S.E.M. of at least three independent experiments. **, *** p<0.01, 0.001 vs. vehicle control; #,##, ### p<0.05, 0.01, 0.001 vs. Day 3.

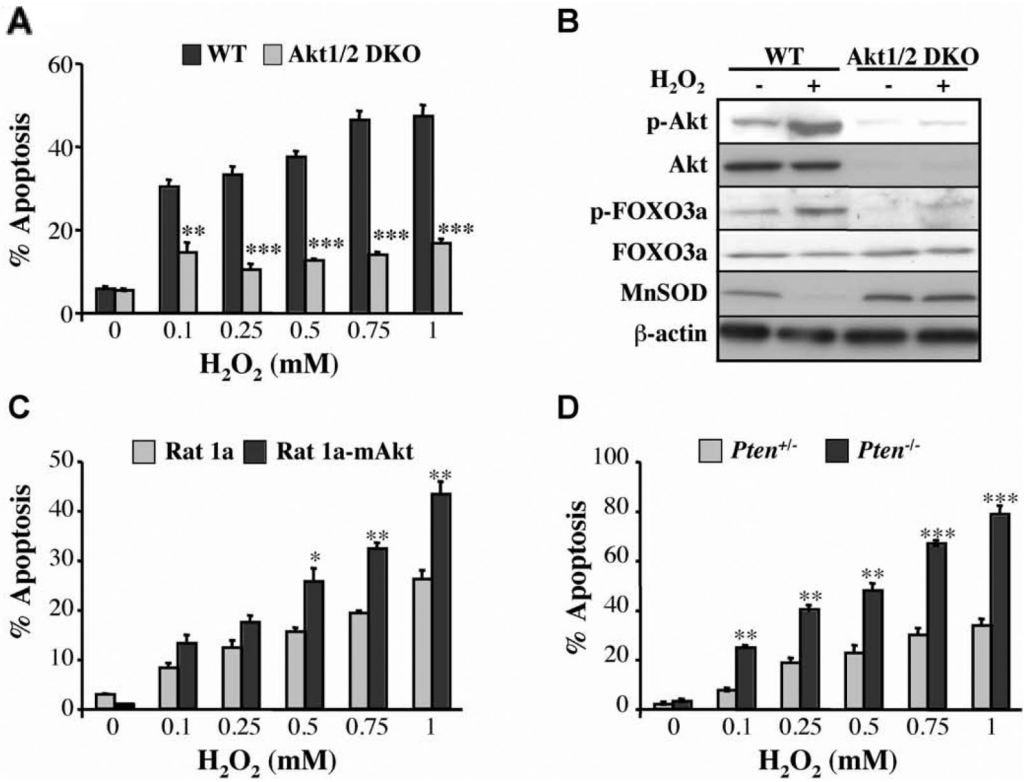

Figure 6. Akt sensitizes cells to oxidative stress mediated apoptosis in a FoxO-dependent manner

A. Akt deficiency exerts resistance to oxidative stress induced apoptosis. DNp53-immortalized WT and Akt1/2 DKO MEFs were treated with increasing concentrations of H_2O_2 (0.1–1 mM) for 2 h, and apoptosis was quantified by DAPI staining. **, *** $p<0.01$, 0.001 vs. WT. **B.** Oxidative stress increases the phosphorylation of Akt and FoxO and reduces the expression of MnSOD. DNp53-immortalized WT and Akt1/2 DKO MEFs were treated with 500 μM H_2O_2 for 10 min, rinsed and then incubated for 2 h prior to cell lysate preparation. The immunoblot shows levels of phosphorylated Akt (Ser473) and FOXO3a (Ser253), total Akt, FOXO3a, MnSOD, and β-actin as a loading control. **C, D.** Activation of Akt sensitizes the cells to H_2O_2-induced cell death. Apoptosis after treatment of Rat1a or Rat1a-mAkt cells with increasing concentrations of H_2O_2 for 2 h. *, ** $p<0.05$, 0.01 vs. Rat1a. **D.** Apoptosis after treatment of Pten+/- or Pten-/- MEFs with increasing concentrations of H_2O_2 for 2 h. **, *** $p<0.01$, 0.001 vs. $PTEN^{+/-}$. All data represent the mean ± S.E.M. of three independent experiments.

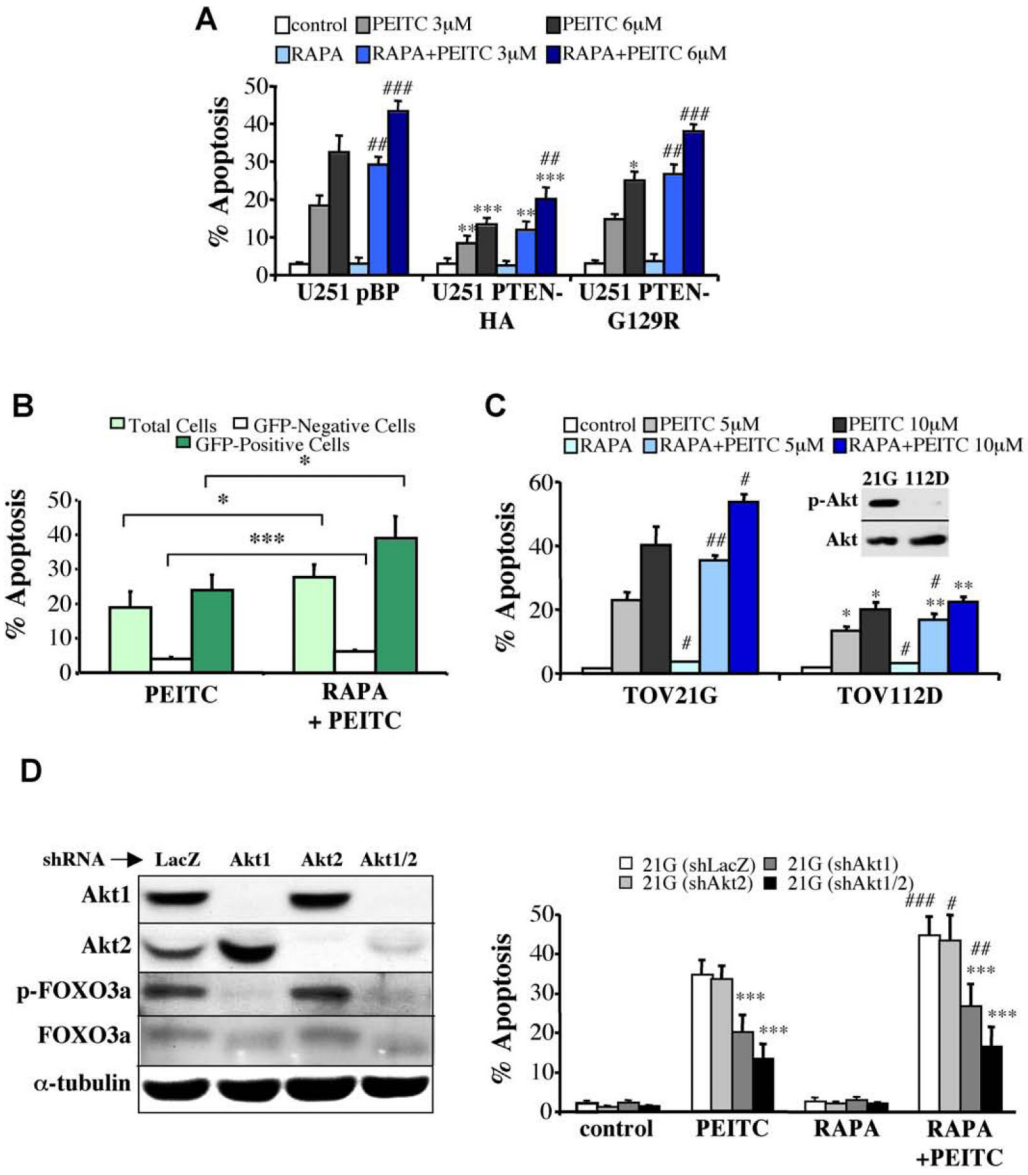

Figure 7. Rapamycin sensitizes cells to PEITC–induced apoptosis in an Akt-dependent manner

A. Pten-deficient, U251 glioblastoma or U251 cells expressing G129R PTEN mutant, are more sensitive to PEITC-induced apoptosis than U251 cells expressing WT PTEN. Rapamycin sensitizes U251 as well as U251-PTEN cells to PEITC-induced apoptosis. *, **, *** $p<0.05$, 0.01, 0.001 vs. control cells (U251 pBP); ##, ### $p<0.01$, 0.001 vs. PEITC in the absence of RAPA. **B.** Preferential killing of cells expressing activated Akt by the combination of rapamycin and PEITC. A mixed population of Rat1a (45.60% ± 1.30% of total cells) and Rat1a-mAktGFP (53.48% ± 1.33% of total cells) was treated with 6 μM PEITC for 6 h after preincubation with 100 nM rapamycin for 3 h. Following incubation, cells were collected and subjected to flow cytometry to assess cell death, as described in Experimental Procedures. The percentage of cell death was calculated within each cell population and is presented as the mean ± S.E.M. of at least three independent experiments, * $p<0.05$, and *** $p<0.001$. **C.** The combination of rapamycin and PEITC preferentially induces apoptosis in ovarian cancer cells with hyperactive Akt. Ovarian cancer TOV21G and TOV112D cells were preincubated with 100 nM rapamycin for 3 h before treatment for

17 h with 5 or 10 μM PEITC. Apoptosis was then assessed by DAPI staining. Data represent the mean ± S.E.M. of at least three independent experiments. Insert shows an immunoblot probed with anti-pSer473 of Akt and with anti-pan Akt in a protein extract from serum-deprived TOV21G or TOV112D cells. *, ** $p<0.05$, 0.01 vs. TOV21G; #, ## $p<0.05$, 0.01 vs. PEITC in the absence of RAPA. **D.** The knockdown of Akt isoforms reduces the susceptibility of TOV21G to apoptosis induced by the combination of rapamycin and PEITC. Left panel: Expression of Akt1 and Akt2 and total Akt activity as measured by FOXO3a phosphorylation in control shLacZ, shAkt1, shAkt2, and shAkt1+shAkt2 TOV21G-expressing cell lines. Right panel: Quantification of apoptosis induced by rapamycin + PEITC in the different knocked down cells, presented as the mean ± S.E.M. of at least three independent experiments. ***, $p<0.001$ vs. TOV21G (sh-LacZ); #, ##, ### $p<0.05$, 0.01, 0.001 vs PEITC in the absence of RAPA.

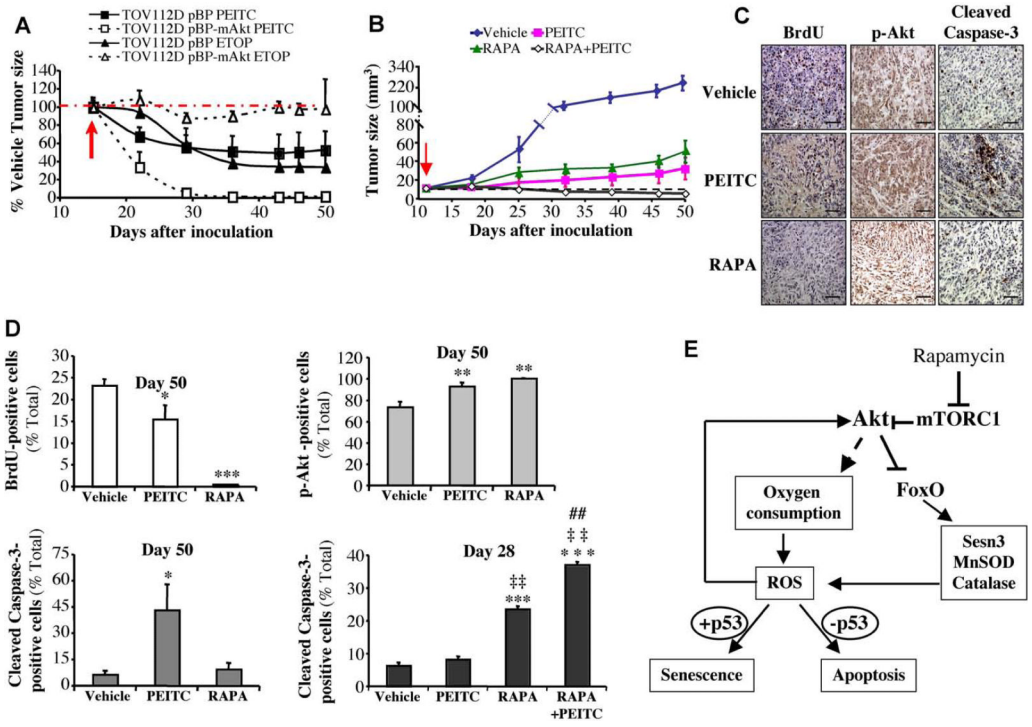

Figure 8. In vivo therapeutic activities of PEITC, and PEITC combined with rapamycin

A. In vivo therapeutic activity of PEITC, compared to etoposide, in mice inoculated with TOV112D ovarian cancer cells or TOV112D (mAkt) cells. Forty two nude mice were injected subcutaneously on both left and right flanks with TOV112D or TOV112D (mAkt) cells, and randomly divided into 3 groups per cell line (14 mice/group, 28 tumors/group) for treatment with PEITC, Etoposide (ETOP) or solvent control. Graph presents the evolution of tumor size respective to the treatment and relative to the control mice. Red arrow indicates the beginning day of the treatment (day 13-post inoculation of the tumor cells). **B.** In vivo therapeutic effect of Rapamycin + PEITC in mice inoculated with TOV21G ovarian cancer cells. Thirty six nude mice were injected subcutaneously on both left and right flanks with TOV21G cells and randomly divided into 4 groups (9 mice/group, 18 tumors/group) for treatment with PEITC, Rapamycin (RAPA), combination of RAPA/PEITC or solvent as a control. Graph presents tumor growth rate in each group. Red arrow indicates the starting day of the treatment (day 13-post inoculation of the tumor cells). **C.** Cross sections of tumors collected from the experiment described in B. At day 50-post tumor cells inoculation, cross sections of tumors were subjected to BrdU staining (*Left* panels), staining with anti-pAkt (*Middle* panels), and staining with anti-cleaved caspase-3 (*Right* panels). Scale bar; 40μm. **D.** Histograms showing the quantification of the positively stained cells in C, and for cleaved caspase-3 staining in tumor sections collected 28 days after inoculation. Results are expressed as the percentage of positively stained cells, and are presented as the mean +/- S.E.M. of percentage of positively stained cells of three sections from three treated mice. Stained and total cells were counted in four random fields of each section. *, **, *** $p<0.05$, 0.01, 0.001 vs. vehicle; ‡‡ $p<0.01$ vs. rapamycin alone. ## $p<0.01$ vs. PEITC alone. E. Schematic illustration summarizing the mechanisms by which Akt activation elevates ROS levels and sensitizes to either senescence or apoptosis. Activated Akt induces ROS by increasing oxygen consumption combined with the inhibition of FoxO transcription factors. FoxOs elevates the expression of ROS scavengers and in particular sestrin3, which is elevated in Akt-deficient cells. ROS could further activate Akt, which in turn further increases ROS levels. The elevation of ROS then sensitizes cells to either senescence or

apoptosis depending on p53 status. Rapamycin, which inhibits mTORC1, further activates Akt, as consequence of the negative regulatory loop inhibition.